Solid-State Proton Nuclear Magnetic Resonance of a Glassy Epoxy Exposed to Water†

R. J. Schadt and D. L. VanderHart*

Polymers Division, National Institute of Standards and Technology, Building 224, Room A209, Gaithersburg, Maryland 20899

Received November 23, 1994; Revised Manuscript Received February 9, 1995⊗

ABSTRACT: A cured epoxy originating from a stoichiometric mixture of a diglycidyl ether of Bisphenol A and 1,3-phenylenediamine has been studied by proton NMR including multiple-pulse techniques. In order to address the question of the uniformity of water distribution based on possible variations in cross-link density, spin diffusion experiments on a dry epoxy were performed over a wide temperature range in order to probe the distance scale of cross-link heterogeneity. The actual experiments measured the minimum distance scale (4 nm) within which sample-wide variations in the multiple-pulse relaxation time, T_{1xz}, are included. Experiments were performed to indicate that these variations in T_{1xz} were not primarily associated with aliphatic versus aromatic protons. Whether the variations in T_{1xz} indicate variations in cross-link density versus fluctuations in local packing in the glass remains an open question. Water chemical shift versus water content was also measured. It was inferred from these data that the majority of the water was molecularly dispersed as opposed to being aggregated into voids. Given that the existence of voids is often invoked in the epoxy literature, the NMR data would limit the volume of any voids to a volume where only one or two water molecules would fit in each void. No evidence was seen in the chemical shift data which would support the idea that there were two different sites with substantially different affinities for water. Also, water line widths were measured at 75 °C for samples of different average water concentrations and relatively uniform concentration profiles. It was anticipated that this measurement would provide a calibration curve whereby the existence of water concentration gradients could be identified for samples of known average water content. This anticipated result was not demonstrated conclusively. Finally, the line-width results are considered as they apply to the behavior of water in the later stages of water uptake.

Introduction

Mechanical properties of epoxies change upon exposure to water. In glassy epoxies, water uptake is thought[1] to involve sites of chemical affinity and voids in the cross-linked polymer network. Both concentration-gradient-controlled diffusion and relaxation-controlled swelling supposedly contribute to the rate and extent of water sorption.[1] It has also been suggested that epoxy consists of a two-phase structure of densely cross-linked regions dispersed in a less cross-linked matrix; thus, certain sorption sites are rendered less accessible because of steric considerations.[2] Therefore, the uniformity of the network cross-link density may also influence the diffusion of water in the glassy state.

An amorphous epoxy polymer network consisting of a diglycidyl ether of Bisphenol A resin cured with 1,3-phenylenediamine has been prepared to investigate its response, below its glass transition temperature (T_g), to water exposure. The extent of cure,[3] dilatometry,[4] tensile properties,[5] dynamic mechanical properties,[6,7] small-angle neutron scattering,[8] electron microscopy,[9] deuteron NMR line shapes of D_2O-exchanged epoxy,[10] calorimetry and influence of water as a plasticizer,[11] water sorption,[12−14] and moisture transport[15] have been reported, but correlations between epoxy morphology and water sorption or diffusion remain vague. In this presentation, solid-state proton NMR methods are employed to inquire about the uniformity of cross-link density and the possibility of multiple sites for water (sites of chemical affinity and voids). Also, a rather simple method, based on water-line-width measurements, is presented for detecting water-concentration gradients. Finally, in light of the NMR data and other published data, some speculative remarks are offered regarding the apparent decrease in translational mobility at the higher water concentrations.

Experimental Section

Stoichiometric amounts of Epon 828 (Shell Chemical Co.) resin[16] (Figure 1) and 1,3-phenylenediamine were heated separately at 70 °C until the 1,3-phenylenediamine crystals melted. The resin was then mixed with the diamine, followed by degassing the mixture under vacuum for 5 min at 70 °C, and poured into a polytetrafluoroethylene-coated mold. Using a heating rate of 5 °C/min, the curing cycle consisted of 2 h at 75 °C, followed by 2 h at 125 °C, and cooling overnight to room temperature. The cured epoxy sheet was nominally 0.5 mm thick and was stored at room temperature in a desiccator prior to NMR sample preparation. NMR samples were prepared from the cured material by cutting disks which fit into a 5 mm diameter glass NMR tube or a Kel-F rotor. Samples were dried (preconditioned) by heating at 75 °C for 48 h under vacuum, after which there was no observable proton NMR Bloch decay line-shape component attributable to water or mobile non-epoxy protons. Samples were exposed to water at 75 °C either in partially evacuated, sealed NMR tubes containing water or by immersion in a water bath. After water exposure, the weight percent water taken up was measured by weighing the sample and by determining the fractional contribution to the 75 °C Bloch decay line shape arising from water protons.

Depending on the particular experiment, 200-MHz proton NMR data were acquired for temperatures from −50 to 200 °C using a Bruker[16] CXP200 NMR spectrometer. Either a Bruker static-sample probe or a Doty Scientific[16] MAS (magic angle spinning) probe was used with a 90° pulse length of 1.5 μs for each NMR probe.

Several radio-frequency pulse sequences were used, none of which is new in concept. We will refer to these sequences by mnemonics, SQ1, SQ2, etc. Wherever multiple-pulse techniques were incorporated into sequences, the MREV-8

* To whom correspondence should be addressed.
† NIST No. 94-14-27.
⊗ Abstract published in *Advance ACS Abstracts,* April 1, 1995.

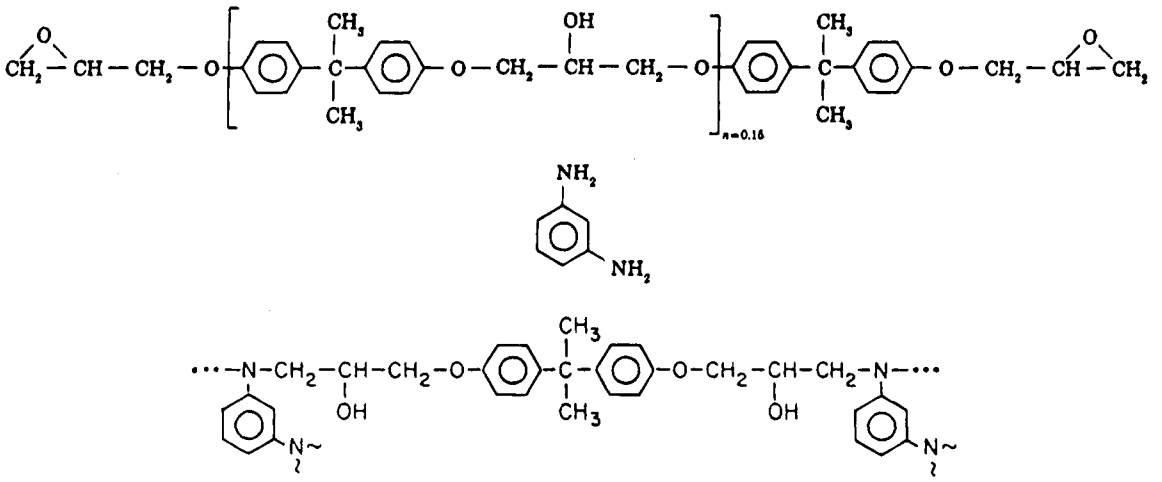

Figure 1. Chemical structure schematic of Epon 828 (top), 1,3-phenylenediamine (middle), and a simplified representation of Epon 828/1,3-phenylenediamine epoxy (bottom). Stoichiometric proportions correspond to 14.5 g of 1,3-phenylenediamine mixed with 100 g of Epon 828.

cycle[17,18] was utilized. One usually applies a train of MREV-8 pulses in any given experiment, sampling data stroboscopically if, in fact, a signal is sampled during such a train. Depending on the preparation pulse preceding this train and the choice of radio-frequency phase for the receiver, one can observe either a free-induction-like signal (Fourier transformed into a spectrum) or a "spin-locked" component of magnetization. The quantity T_{1xz} characterizes the time constant for relaxation during such spin locking. T_{1xz} measurements were made at about 4–5 kHz from resonance (so the chemical shift offset Hamiltonian would dominate the pulse-error Hamiltonian for good locking[19]); moreover, static samples were utilized (we have seen spurious contributions to T_{1xz} arising from sample spinning frequencies).

The first two sequences to be discussed are spin diffusion experiments designed to yield a distance scale associated with variations in proton relaxation rates in a dry epoxy. The first sequence, SQ1, is a "T_{1xz} preparation–spin diffusion–T_{1xz} observation" experiment.[20] The NMR pulse sequence consisted of $[45_{-y}-(\text{MREV-8})_n-45_y-t_{sd}-45_{-y}-[(\text{MREV-8})_m(=\text{obs})]-T-180_\phi-1\text{ ms}-45_{-y}-(\text{MREV-8})_n-45_y-t_{sd}-45_{-y}-[(\text{MREV-8})_m(=\text{obs})]-T-]$ with alternate adding and subtracting of data and nonquadrature phase detection. Radio-frequency pulses are indicated by their flip angles, with the subscript referring to their relative phases; i.e., x, y, $-x$, and $-y$ respectively correspond to phases 0°, 90°, 180°, and 270°. The spin diffusion time is t_{sd}, and T is the time between experiments. The latter is chosen to be at least $5T_1$, where T_1 is the longitudinal proton relaxation time. The 180° pulse preceding alternate acquisitions is phase cycled over all four phases. This pulse, along with the 1 ms delay, which is long compared to the transverse proton relaxation time, T_2, and short compared with T_1, allows us to add and subtract alternate scans and preserve a "zero baseline" in these spectra. The latter is important since duty cycle considerations often prevent the observation of the entire T_{1xz} decay; hence, a knowledge of the "zero-signal" position is necessary for properly evaluating the extent of decay.

SQ2 is simply SQ1 where an MREV-8 spectrum observation is substituted for the T_{1xz} observation. The sequence for SQ2 is $[45_{-y}-(\text{MREV-8})_n-45_y-t_{sd}-90_x-[(\text{MREV-8})_m(=\text{obs})]-T-180_\phi-1\text{ ms}-45_{-y}-(\text{MREV-8})_n-45_y-t_{sd}-90_x-[(\text{MREV-8})_m(=\text{obs})]-T-]$. Application of both SQ2 and SQ1 for a given choice of t_{sd} allows one to correlate chnages in T_{1xz} decays with changes in the kinds of protons contributing to the T_{1xz} decays.

SQ3 is a spin diffusion experiment intended as a crude probe of water distribution. This is an experiment in which the rate of spin diffusion between water and epoxy protons is measured, starting from an initial condition where a major portion of the water polarization is saved and the epoxy polarization is quenched. The SQ3 sequence is $[90_x-100\ \mu s-180_y-100\ \mu s-90_{\pm x}-t_{sd}-90_\phi(=\text{obs})-T-]$. Data are alternately added and subtracted; the phase ϕ is advanced every even-numbered scan and properly coordinated with the receiver phase.

The final sequence, SQ4, was used to measure T_2 for water protons and to collect the echo decay as a function of transverse decay time. The SQ4 sequence is $[90_x-nT_r-180_y-nT_r-90_{\pm x}(=\text{obs})-\text{T}-]$, where T_r is a rotor period and n is an integer. The echo separation was chosen to be an integral number of rotor periods in case the water protons experienced any nonvanishing dipolar interactions. This is the sequence utilized to measure T_2 and to ascertain whether the water line width was a function of the echo time.

Finally, "M_0" signals or spectra are mentioned. These serve as reference points for data from the above sequences. These M_0 signals are the responses of Boltzmann equilibrium spins to the corresponding modes of signal observation in the above sequences. These modes include Bloch decay spectra, MREV-8 spectra, and T_{1xz} decays.

Chemical shifts (in ppm) of water protons in epoxy were measured relative to a tiny piece of poly(dimethylsiloxane) inserted into the middle of the sample region. The proton chemical shift of poly(dimethylsiloxane) (cyclic tetramer) relative to tetramethylsilane (TMS) is reported to be 0.09 ppm;[21] the measured values we report are relative to TMS and are adjusted by this value. We also measured the chemical shift between TMS in a capillary and poly(dimethylsiloxane) surrounding the capillary; results were consistent with the 0.09 ppm shift.

Temperatures in the NMR probe at the sample location were determined in separate experiments, using a partially evacuated, sealed glass capillary containing either ethylene glycol (for temperatures of 20 °C and above) or methanol (for temperatures below 20 °C). Sample temperatures were deduced from the chemical shift separation[22–24] either between the methine and hydroxyl protons of ethylene glycol or between the methyl and hydroxyl protons of methanol depending on the temperature range of interest. For MAS experiments, temperatures between 20 and 110 °C were also determined at the sample location at various magic angle spinning speeds by using an ethylene glycol capillary placed inside a sample rotor packed with precipitated sulfur (112 °C melting point).

Results and Discussion

Inquiry into Cross-Link Density Variation. Differences in cross-link density should result in different mobilities, which, in turn, should give rise to a dispersion of relaxation times. In particular, during MREV-8 irradiation, spin diffusion is suppressed. Thus, to a first approximation, each proton relaxes at its own rate during a T_{1xz} decay; those decay rates depend mainly on spectral densities of motions at mid-kilohertz frequencies.[25,26] Hence, at some point part of the way

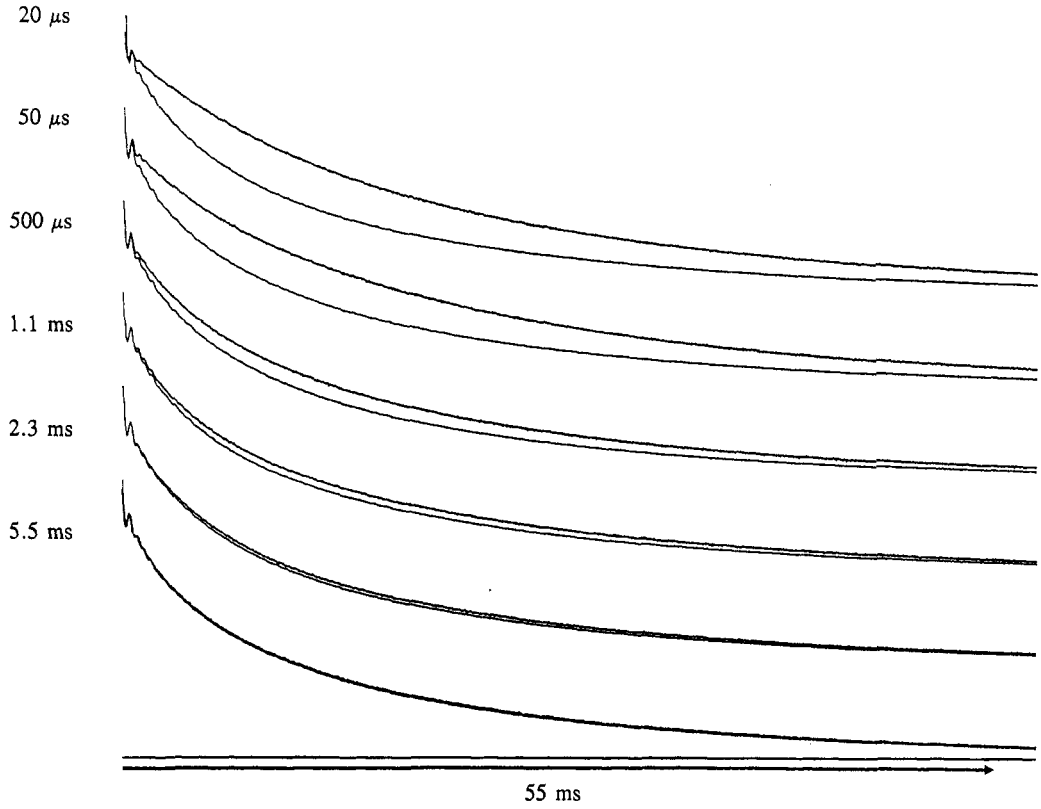

Figure 2. Data using the SQ1 sequence ($n = 350$, $m = 1500$) for the dry Epon 828/1,3-phenylenediamine at −40 °C. T_{1xz} profiles at each of the given spin diffusion times are compared with scaled M_0 profiles. The time scale of the profiles is indicated (>55 ms) along with the baseline appropriate to the bottom pair of overlapping profiles).

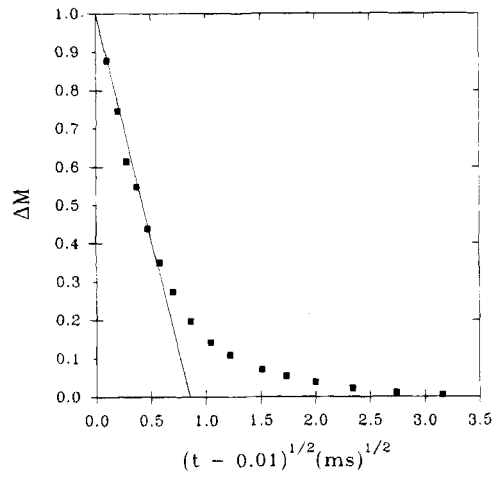

Figure 3. Analysis of the data illustrated in Figure 2. Difference (ΔM) between T_{1xz} (M_0) and T_{1xz} (spin diffusion) profiles, i.e., from Figure 2 at point 300 along the time axis (out of 1500 total points in each plotted profile). The line indicates a fit to the initial slope of the data points, and the time scale associated with equilibration, via spin diffusion, after imposition of the initial spin polarization gradient, is represented by the intercept of this line with the time axis.

through a T_{1xz} decay, polarization gradients are expected to exist based on a fundamental difference in mobility for any of the following reasons: (a) protons within each repeat unit in a fully crosslinked region consistently exhibit different mobilities (e.g., aliphatics vs aromatics), (b) protons are near un-cross-linked points, (c) protons are in regions of lower **average** cross-link density (e.g., have generalized larger-amplitude motions, supposing motions require cooperativity), and/or (d) protons are in the immediate vicinity of a region of lower packing density, assuming a glassy material contains local density variations.

For a dried, nonspinning sample, SQ1 and SQ2 were applied. In the preparation portion of these sequences, a polarization gradient based on T_{1xz} differences in the epoxy was prepared using 13.44 ms of irradiation. Then the progressive disappearance of this gradient was followed as a function of spin diffusion time. Temperature was varied from −40 to −200 °C to search for a temperature at which T_{1xz} contrast would be most sensitive to mobility differences associated with average cross-link density variations. Using SQ1 at −40 °C, recovery via spin diffusion to the equilibrium T_{1xz} profile (Figure 2) was typical of other temperatures and was about 80% complete in 1 ms, 90% complete in 2 ms, and 99% complete in 9 ms (Figure 3). Thus, variations in T_{1xz} were indeed seen, but the generated polarization differences disappeared rather quickly. Since we hoped to measure the distance scale over which cross-link density was uniform and since variations in cross-link density are not the only possible contributions to a T_{1xz} dispersion, we tried to gain additional information about the origin of the gradient produced.

Parallel SQ2 experiments, for comparison to SQ1 results using the same preparation time and the same set of spin diffusion times, were then carried out in order to test whether the initial gradient was based on intrinsic mobility differences between aromatic and aliphatic protons. In Figure 4, after 50 μs of spin diffusion, the spin diffusion line shape was indistinguishable from the equilibrium line shape. In view of the fact that aliphatic protons contribute more strongly to the upfield side of the nonspinning line shape, even though there is substantial overlap for the aromatic and aliphatic line shape components, we adopt the qualitative conclusion that aromatic/aliphatic polarization

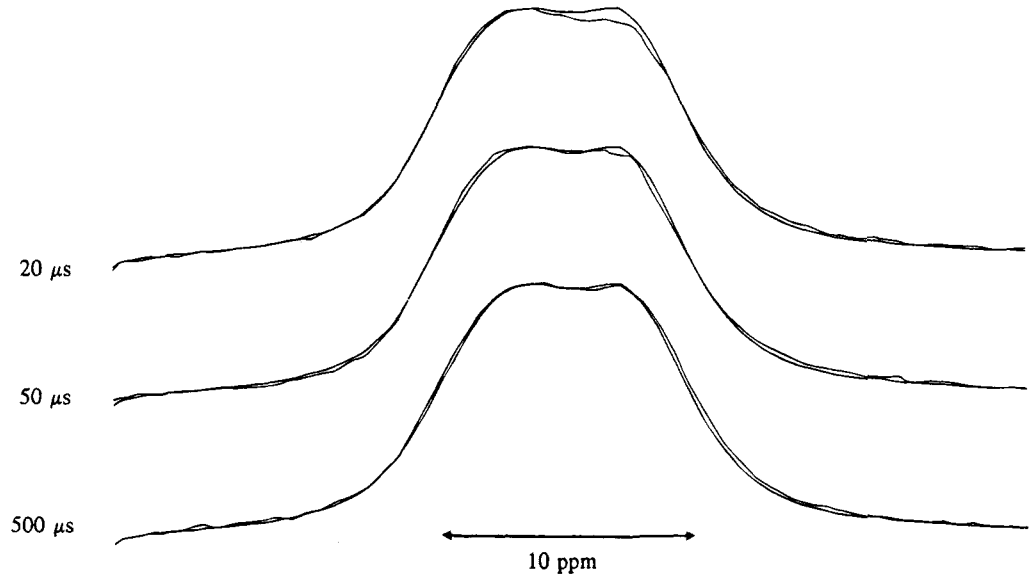

Figure 4. Data using the SQ2 sequence for dry Epon 828/1,3-phenylenediamine at −40 °C. Scaled MREV-8 line shape (M_0) compared to MREV-8 line shape acquired with T_{1xz} preparation (same as employed in T_{1xz} profile acquisition (Figure 2)), spin diffusion time as indicated, and MREV-8 spectral readout. A slight polarization bias is indicated at short spin diffusion times by the reduced line-shape intensity of the right peak, associated primarily with aliphatic groups, compared to the line-shape intensity of the left peak which is associated primarily with aromatic groups. By 50 μs, aromatic and aliphatic polarizations are near equilibrium. Thus, the data of Figure 3 mainly monitor the dissipation of gradients other than aliphatic/aromatic proton polarization gradients.

gradients are very minor after 50 μs of spin diffusion. Hence, most of the initial polarization gradient can be identified with mobility differences associated with variations in crosslink density or with variations in intermolecular potentials as opposed to systematic mobility differences between aromatic and aliphatic protons. Assuming a spin diffusion coefficient of 5×10^{-12} cm^2/s,[27,28] the rate of recovery of the T_{1xz} profile implies that the inhomogeneity in mobility sensed in this experiment is uniform on a scale of 4 nm and larger. This scale is too small to associate with phase separation, except perhaps at the very late stages of crosslinking. This result is also consistent with a uniform distribution of cross-links on a scale greater than 3 nm observed for a closely related epoxy via small-angle neutron scattering.[8]

We do not wish to claim that our results definitely give a distance scale for cross-link variations. We have recently made similar (unpublished) measurements on un-cross-linked glassy polymers and have obtained similar results. Hence, for us, the important result is that there was no evidence of a distance scale, larger than 4 nm, which possessed a mobility gradient. We did not pursue this experiment using less stoichiometrically mixed epoxies since most epoxy formulations are close to stoichiometric.

We decided to apply a rather crude test for the uniformity of water concentration throughout the epoxy network. If the suggestion is true that cross-link density variations are responsible for water first penetrating the regions of lower cross-link density,[2,14,15] then, especially at the lower water concentrations, these local concentration fluctuations should be present. We chose an epoxy sample with 0.8 wt % water to probe the water distribution. The concept of the experiment was the following: Prepare an initial polarization where only the water protons have polarization. Then, by spin diffusion, let the water polarization flow into the epoxy–proton reservoir until polarization flow ceases. The spin diffusion line shape in this asymptotic time regime will then indicate what a fraction of the epoxy protons is in "spin diffusion contact" with the water; i.e., any regions devoid of water protons, and not within the spin diffusion range from water protons, will not share any polarization with the water protons. If we define R to be the ratio of water to epoxy intensity contributions to the proton line shape, then the fraction, f, of the epoxy protons in "spin diffusion contact" with the water protons is given by

$$f \approx R(M_0)/R_{sd} \tag{1}$$

where $R(M_0)$ and R_{sd} are respectively evaluated for the M_0 (equilibrium; no initial polarization gradient) and the asymptotic spin diffusion line shapes. Figure 5 shows the experimental results taken at 50 °C using SQ3. This temperature was selected as a compromise considering two trends. Spin diffusion between water and epoxy protons becomes more efficient at lower temperature; however, the water line width also broadens, thereby effectively reducing signal to noise. For $t_{sd} = 25$ μs, no epoxy signal is evident; at $t_{sd} = 5$ ms, much of the polarization transfer has occurred; yet R is still much larger than $R(M_0)$ as can be seen from the M_0 spectrum, which is overlaid and scaled down by a factor of about 200. At $t_{sd} = 25$ ms, one gets the lower, noisier trace of Figure 5, shown together with the scaled M_0 spectrum. The R values for the two lines are certainly comparable; however, signal-to-noise considerations limit the precision of this statement. We believe these data support the claim that $R_{sd} \leq 1.5R(M_0)$, i.e., $1 \geq f \geq 0.67$. Hence, at least $^2/_3$ of the epoxy protons are in spin diffusion contact with the water. This is not a very precise statement and leaves room for considerable concentration variations. Since the sensitivity of this experiment goes approximately as the water concentration squared, we considered raising the concentration. However, we decided against this because the postulate we were exploring implies that water gains wider access as the concentration of water increases. Consequently, proof of a uniform distribution at higher water concentrations is not very valuable in this context.

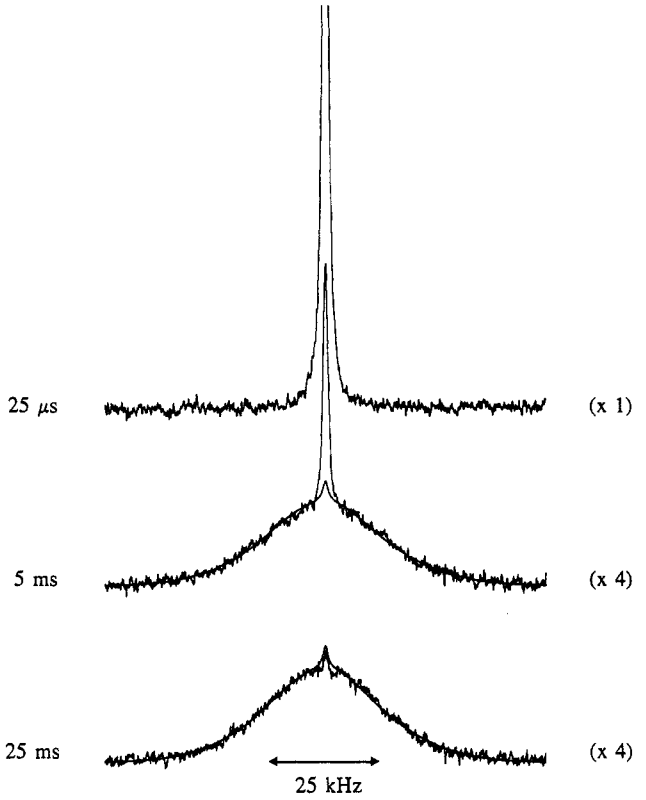

Figure 5. Epon 828/1,3-phenylenediamine at 50 °C with 0.8 wt % water. Scaled Bloch decay line shape (M_0) compared to the line shape acquired with T_2 selection of water (single Carr–Purcell echo with 100 μs delay time before restoration of Zeeman magnetization) followed by spin diffusion time (t_{sd}) as indicated. Line broadening of 150 Hz is applied prior to Fourier transformation. Vertical amplification factors, based on spectra normalized to the same number of scans, are shown on the right.

A final comment about this experiment is that one is tempted to associate a distance scale with the shortest t_{sd} for which the asymptotic condition is reached. But this distance scale depends on the assumptions about the water distribution. Qualitatively, if water is *excluded* from some regions, then an experimental result where $f < 1$ means that those regions are larger than twice the *spin* diffusion distance over this shortest t_{sd}. (For $t_{sd} = 25$ ms, implied distances would then be in excess of 8 nm.) On the other hand, if concentration varies but no region is devoid of water, then it is fair to expect that water diffuses through all the regions within the translational diffusion distance characteristic of this "shortest t_{sd}". Since there is no way of knowing where the polarization exchange between water and epoxy protons occurs, the conservative interpretation is that, if $f < 1$, then concentration gradients must exist over dimensions larger than twice the translational-diffusion distances. (For $t_{sd} = 25$ ms and $D = 2 \times 10^{-8}$ cm^2/s, distances would exceed 1 μm.) The conservative interpretation, then, is that this experiment represents a test for uniformity of water concentration on the micrometer scale. It should be mentioned that the 25 ms spin diffusion spectrum in Figure 5, owing to the weak total intensity it possesses, is very susceptible to distortions arising from extraneous background signals from the probe (the water signal in this spin diffusion spectrum is less than 10^{-4} times the total M_0 signal). The line shape shown has been corrected carefully for background signals.

As an aside, the mechanism for polarization transfer between water and epoxy protons could, in principle, include chemical exchange as well as spin exchange arising from transient dipolar interactions. The exact mechanism for polarization transfer is not crucial to the above arguments. Nevertheless, relative to the rates of chemical exchange between water protons and hydroxyl or amine protons, deuteron results[10] indicate that such exchange is slow on the microsecond time scale; moreover, we observe that the strength of the water signal at 70 °C correlates well with the known amount of water in the sample. Hence, the "pool of mobile protons" does not include the hydroxyl and amine protons; i.e., chemical exchange is also slow on the 100 μs time scale.

Inquiry into Multiple Sites for Water. At least two different kinds of sites are postulated for water in epoxy: "voids" and sites of chemical affinity, e.g., hydroxyl groups formed in cross-linking or amide groups associated with un-cross-linked sites. (For the stoichiometry of the reactants chosen for this epoxy, the hydroxyl groups should greatly outnumber the amide groups.[3,15]) One of the strongest arguments for voids is that, in the range of 0–1 wt % water uptake, a water molecule produces about half the lattice expansion that it would have produced in the range 1–3.4 wt %.[13] In this latter range, the volume increase per water molecule is close to the average volume per molecule of bulk water. The inference drawn is that the first water taken up shows a preference for voids, even though many authors who invoke voids do not speculate on how large these voids are. Admittedly, when we thought of voids, we imagined spaces sufficiently large to contain several water molecules. For example, a 2 nm diameter spherical void could contain about 140 water molecules. From a thermodynamic viewpoint, we had trouble with this concept of early void filling because we expected that, energetically, water should prefer hydrogen-bonding sites, e.g., hydroxyl groups, over voids containing other water molecules.

The simplest way to distinguish multiple sites for water is to identify different sites on the basis of distinct chemical shifts for water protons at each site. Figure 6 shows temperature-dependent line shapes for a static sample containing 3.2 wt % water. At 75 °C, the narrow water signal can be easily distinguished from the broader epoxy signal. The relative integrals of these two components also agree very well with the amount of water determined gravimetrically. Yet, there is only one water resonance visible. Thus, at 75 °C, we conclude either that there is only one site for water or that, if there are multiple sites, the protons of water are in the fast-exchange limit; i.e., the residence time of the water at any one site is very short compared to the inverse of the resonance-frequency difference for water at the various sites.

One simple approach for revealing multiple sites in the fast-exchange limit is to lower the temperature with the hope of reducing the exchange rate between possible sites so that distinct, site-dependent chemical shifts appear. As can be seen from the other spectra in Figure 6, this approach failed because, as temperature is decreased, the Bloch decay water line widths become broader. At about −20 °C, the water protons can no longer be distinguished from the epoxy signals. At no point is there evidence for multiple shifts or multiple line widths for water. (Line shapes were also taken using MAS. No chemical shift differences were revealed

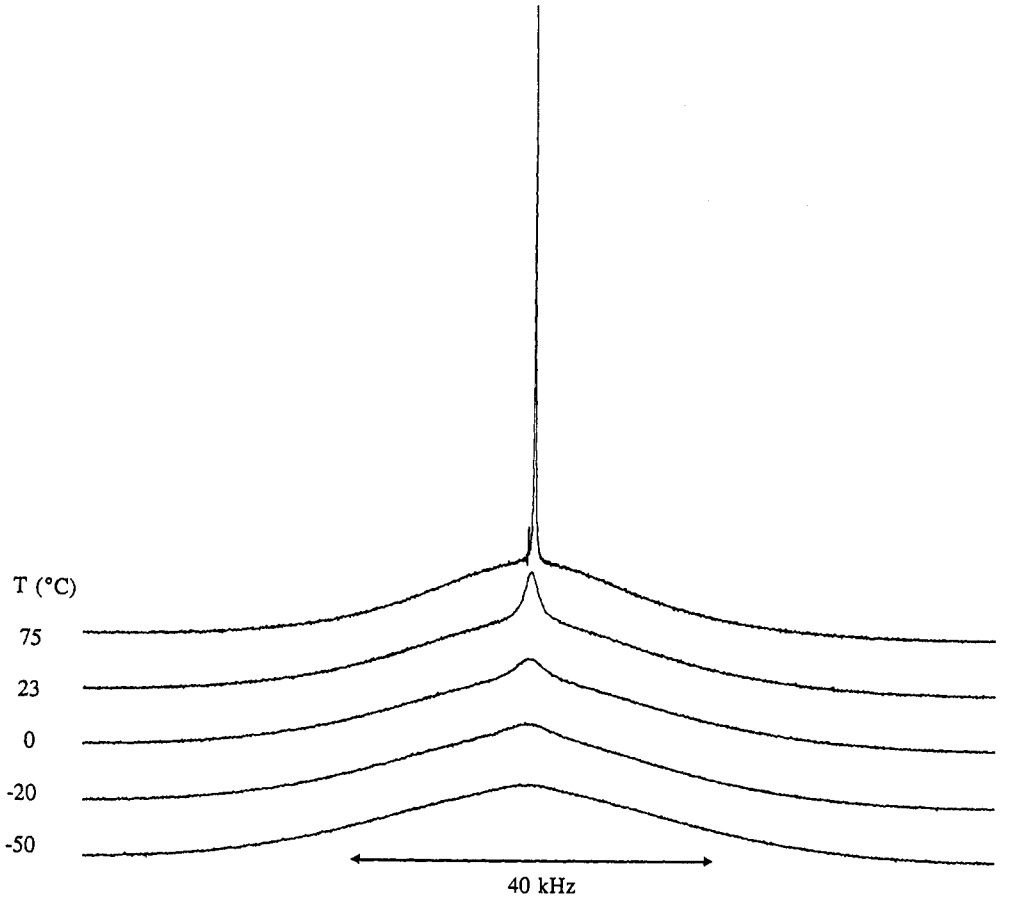

Figure 6. Proton NMR Bloch decay line shape (static sample) as a function of temperature for Epon 828/1,3-phenylenediamine with 3.2 wt % water.

in these line shapes either; however, we did find that it was necessary to limit MAS frequencies to 2 kHz or less to avoid narrowing certain epoxy–proton resonances. For example, at a 4 kHz MAS frequency, one definitely generates a narrowed signal from a small subset of protons in the epoxy network, and it is hard to separate this contribution cleanly from that of the water.) Thus, in searching for multiple sites for water, we discarded the approach of reducing temperature, deciding rather to work at higher temperatures, like 75 °C, where the water resonance can be easily distinguished from epoxy line shape. Therefore, for the other approaches undertaken in probing for multiple sites, we assume that water is in the fast-exchange limit.

One can generate a useful perspective, with respect to any fast-exchange process, by considering how far a water molecule will travel at 75 °C in this epoxy if it diffuses isotropically with a diffusion constant, D, of 2×10^{-8} cm^2/s, the diffusion constant deduced from water uptake curves[14,15] (Figure 7). On the time scale of 1 ms, which is on the order of T_2 for the water, the water will travel about 100 nm [$=(6Dt)^{1/2}$]. It is likely that, if multiple sites exist, they have a uniform density on this scale which is several times the 4 nm scale of motional heterogeneity described in the preceding section.

In the fast-exchange limit, the chemical shift of a water molecule is a qualitative indicator of whether it is spending a major portion of its time aggregated in voids containing several water molecules. It is known that the chemical shift of bulk water is influenced by its substantial opportunities for hydrogen bonding. In fact, at ambient temperature, there is a downfield shift of 4.25 ppm associated with the condensation of water from the gaseous to the liquid state.[29] Also, for water dispersed in small quantities in organic solvents, one generally sees an upfield shift of 2–3 ppm relative to bulk water.[30,31] There is also a slight upfield shift with increasing temperature for bulk water, ostensibly because thermal energies compete with hydrogen bond formation. It was in consideration of this latter point that we measured the chemical shift of water in epoxy (using MAS) as a function of water uptake at a *fixed temperature* (75 °C) rather than as a function of temperature. Results are shown in Figure 8. We chose to make these measurements at 75 °C for the following reasons: (a) the mobile component of the Bloch decay line shape correlates with water uptake, (b) 75 °C is at least 30 °C below the calorimetric T_g including that of the wet state (differential scanning calorimetric T_g is approximately 145 °C (dry); 110 °C (3.2 wt % water)),[9,11,15] and (c) 75 °C matched the sample drying (preconditioning) and water exposure temperature.

In Figure 8, the chemical shift of water at the lowest water content, 0.4 wt %, is 2.53 ppm. This level of water falls into the range where, presumably, void filling is important. Yet, the chemical shift is 1.8 ppm upfield, relative to the shift for bulk water at 75 °C (4.30 ppm[32]). Such an upfield shift is typical of water which is mainly dispersed on a molecular basis, rather than aggregated into regions where several water molecules would interact with one another.

Aside from the foregoing qualitative remark about water being dispersed, the linear dependence of the chemical shift on water content suggests two other points related to probing for the existence of voids containing several water molecules. First, if, as the volumetric expansion data suggest,[13] water, up to about 1 wt %, has a higher probability of residing in voids than

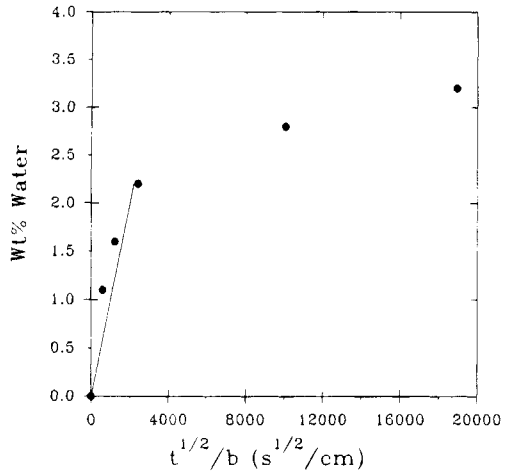

Figure 7. Water uptake of Epon 828/1,3-phenylenediamine at 75 °C. The line is intended as a visual aid corresponding to a water diffusion (initial sorption) coefficient of 2×10^{-8} cm²/s. The time axis is normalized to sample thickness b (cm).

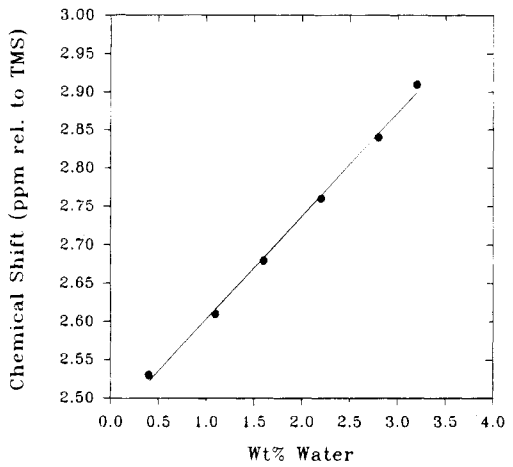

Figure 8. Chemical shift (ppm relative to tetramethylsilane (TMS)) at 75 °C of water protons in Epon 828/1,3-phenylenediamine as a function of 75 °C water uptake. No apparent break in positive slope and linearity of the data points is indicated.

it does at higher water contents, then the chemical shift should reflect that. There is no break in slope near 1 wt % water in Figure 8; moreover, the slope of the data has the wrong sign if the state of aggregation solely determines the chemical shift and if, on average, water were spending a larger fraction of its time in a dispersed, as opposed to an aggregated, state at the higher water contents. The second point is rather weak in that it depends on several qualifying factors (vide infra). Nevertheless, there is no evidence for, say, two different, comparably-abundant sites for water with different associated chemical shifts and considerably different affinities for water. If this situation prevailed, then the first water taken up would prefer those sites of stronger affinity; hence, the exchange-averaged chemical shift would be biased toward the shift typical of those sites. At higher water contents, after the sites of stronger affinity approach saturation and the sites of weaker affinity become more populated, the exchange-averaged chemical shift would move toward the chemical shift of the less favored sites. If the chemical shift of water were determined solely by the population-weighted average shift over two sites, then Figure 8 would be quite nonlinear in contradiction to what is observed.

For water dissolved in aprotic polar solvents like dioxane, dimethyl sulfoxide, acetonitrile, tetrahydrofuran, and dimethylformamide, it is quite common at low water levels to see the chemical shift of water increase in approximately linear fashion with water concentration[30,31] as is observed in Figure 8. Moreover, in solvents like dioxane and tetrahydrofuran, the slope of the shift versus weight percent water[31] is comparable to what is observed in this epoxy. In these solvents, the shift of water is explained on the basis of an increasing probability that water will hydrogen bond to itself as its concentration in the solvent increases. Similarly in our opinion, that is the most likely cause for the change in chemical shift observed in Figure 8. Thus, in Figure 8 we see no evidence for multiple sites for water. In addition, water seems to be very dispersed in the sample and not aggregated. Therefore, we rationalize our data and the lattice-swelling data[13] by concluding that the voids occupied by the water at low water concentrations are not large enough to allow much water–water hydrogen bonding. In other words, the term voids takes on a meaning closer to that of "free volume", i.e., a small space in which one or two water molecules might fit.

Miscellaneous Observations. As will be illustrated presently, water line widths, i.e., the full width at half-height (fwhh), measured at a fixed MAS frequency, become narrower as the concentration of water increases. Line widths also become narrower as MAS frequency increases. Moreover, at a given MAS frequency, the relationship $\pi T_2 = (\text{fwhh})^{-1}$ is found to be a good approximation, where fwhh has units of hertz. Thus, the existence of water-concentration gradients through the thickness of an epoxy disk should be accompanied by a corresponding distribution of line widths or T_2's. We looked for a distribution of T_2's in a sample immersed in water for about 20 min at 75 °C. This sample absorbed about 0.8 wt % water from its initial dry state; hence, sizable gradients were expected to be present even though the time between removal from the bath and the NMR analysis at 75 °C was slightly in excess of an hour. Using the SQ4 sequence, we looked for the water resonance in the transformed echo to become broader as the time between pulses was incremented. Partly for reasons of signal-to-noise limitations, we were not able to observe any increase in line width as a function of the pulse spacing. When we modeled this experiment mathematically, it became evident that a change in line width as a function of echo time is not a very sensitive way to identify a dispersion in T_2; e.g., in this case, when the range of T_2 is only a factor of 2, then the line width changes only by 4% for a 4-fold reduction in echo amplitude.

In Figure 9, line-width data are given for water as a function of its average concentration. Two pairs of curves are presented. The choice of data is based on rather simple mathematical modeling whose results indicated the following. If one measures the difference in water line widths from two samples with identical average water concentrations, one sample possessing concentration gradients and the other with a uniform concentration profile, this line-width difference should be a few times larger than corresponding line-width differences observed as a function of echo time (and over a reasonable attenuation range) in a T_2 experiment. Moreover, the inconvenience of having to compare line widths on samples with two preparation histories is partly offset by having better signal-to-noise compared

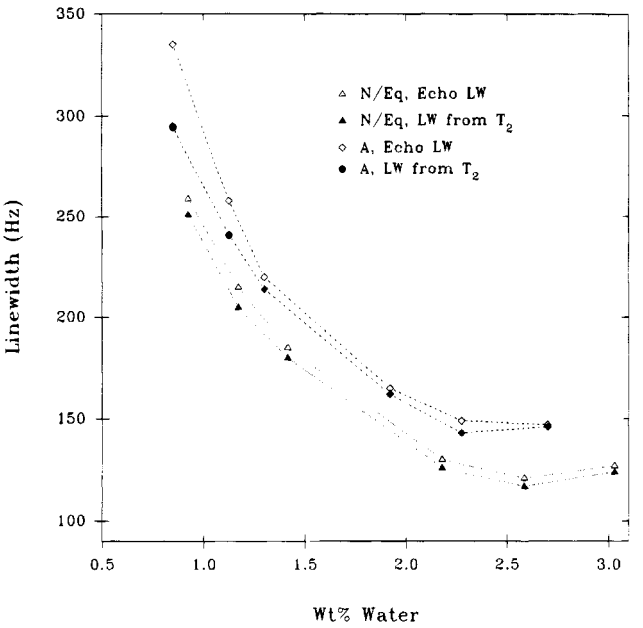

Figure 9. Water line width (1.7 kHz magic angle spinning) at 75 °C as a function of water uptake for a single Epon 828/1,3-phenylenediamine sample which is sequentially exposed to cycles of water immersion, NMR analysis, annealing, and further NMR analysis. The "A" data are taken after the annealing step; the "N/Eq" data are taken after the immersion step. Owing to the existence of larger water-concentration gradients at the time of the N/Eq measurements, relative to the A measurements, the N/Eq curve should yield smaller line widths for a given water content. Note that water line widths (fwhh) derived from a single Carr–Purcell rotor-synchronized echo, using the SQ4 sequence, compare favorably with water line widths derived from T_2 decays; i.e., fwhh = $1/\pi T_2$ is approximately satisfied. Lines connecting the points are for visual clarity only.

to line-width measurements at the longer echo times in a T_2 experiment.

The two pairs of curves in Figure 9 are intended to illustrate (a) a general reduction in line width (or increase in T_2) with increasing water concentration and (b) an increase in line width upon annealing at 75 °C at a fixed concentration, where annealing reduces water concentration gradients in the sample. The data of Figure 9 pertain to a single sample which, after drying at 75 °C, has been treated to a sequence of cycles, each cycle consisting of (a) water exposure for a variable time at 75 °C in a sealed tube from which air had been removed, (b) gravimetric analysis at ambient temperature followed by NMR line shape and T_2 measurements at 75 °C, (c) thermal annealing for at least 25 h (annealing times up to 68 h were used at lower water contents) in a small, sealed, initially evacuated tube at 75 °C, and finally (d) a second round of gravimetric and NMR analysis. We will refer to the samples analyzed after the immersion step as "N/Eq" (nonequilibrated); samples analyzed after annealing are called "A". We recognize that 25 h of annealing is not sufficient to bring about true equilibrium; normally in a water uptake experiment, about 75–80% of the equilibrium water would be absorbed in 25 h.[12-15] However, 25 h should be adequate to substantially reduce gradients. Furthermore, since immersion and annealing are conducted stepwise, gradients in the A samples should be modest.

In Figure 9, the data for the A samples have line widths greater than those for N/Eq samples, as expected, given that the latter samples have larger gradients. Note, however, that if one considers pairs of points which are related chronologically, then the average water content in the A samples is always lower than that in the N/Eq samples. The reason for this is that we did not want further water uptake during annealing. Since we did not know the relative humidity corresponding to no further water uptake, we elected to anneal samples in a sealed tube of small volume and to tolerate some water loss until the vapor pressure in the tube reached a point where further loss was minimal. (Given the volume of the sample and the volume of the tube, we estimate that a water loss of 0.2–0.3 wt % is required in order to generate inside the tube the equilibrium vapor pressure over pure water at 75 °C; this is consistent with the apparent water loss at the higher water contents.) In Figure 9, at the lower water contents, the line-width differences, interpolated to the same average concentrations, are about 60 Hz (about 30 Hz from T_2 measurements); however, at the higher water contents, the difference in line widths, measured directly or via T_2, remains at about 20 Hz. We expected the two data sets to converge at the higher water contents. It is particularly puzzling that the N/Eq line width at 3.0 wt % moisture (where this sample was immersed at 75 °C for 15 days and should have come very close to equilibrium) is still about 20 Hz smaller than the A line width at 2.7 wt % water following a 26 h annealing. By itself, such a line-width increase might be attributed to a loss in average water content. The puzzling issue is that neither the A nor the N/Eq data support any important dependence of line width on concentration in the range from 2.3 to 3.0 wt % water. Hence, the observed line-width increase upon annealing is hard to rationalize simply on the basis of a water concentration profile change. Therefore, we are unsure of the correct interpretation of the A and N/Eq data difference. There is a self-consistency to the data which prevents our dismissing the data difference as uncertainty in the measurements. At the same time, we cannot with confidence claim that the difference between the A and N/Eq curves is dominated by the size of water-concentration gradients. One possibility is that paramagnetic oxygen is present in systematically greater amounts in the A samples, thereby increasing the line widths via enhanced relaxation. (This might happen if, for example, oxygen, absorbed in the preceding analysis step, preferentially partitioned itself out of the epoxy phase and into the aqueous phase during immersion but had no opportunity to do that during annealing where water is absent.) In any case, the data of Figure 9 should be viewed primarily as the approximate dependence of line width on water concentration.

The monotonic decrease in line width with water concentration suggests that the mobility of water increases with increasing water concentration. At the same time, if one tries to fit the typical water uptake curve to a fixed translational diffusion coefficient, one invariably underestimates the time required to reach equilibrium.[12,13] That is to say, it appears that the diffusion coefficient for water is getting smaller as water concentration increases. The reason for this behavior is still a matter of debate; the role of slow, sub-T_g lattice expansion,[12] chemical reactions with oxygen,[12] and heterogeneous access for water owing to cross-link density variations[13] are some of the alternative explanations which avoid requiring that water diffusion slows as water content increases. The relationship between water line width and its translational diffusion coefficient is ambiguous in the sense that, in addition to

translational mobility, line width is sensitive to the isotropy and dynamics of reorientational motion.[32] Hence, it is possible, in principle, that translational motion slows down while rotational motion becomes more facile or more isotropic, with the result that line width decreases. In the case of epoxy, one may rationalize this situation by invoking greater isotropy of motion, owing to the expansion of the glass upon water uptake; i.e., water can reorient more isotropically in the implied larger cavities. Thus, without further measurements in which the relative contributions of translation and rotation to line width are separated, we cannot conclude whether the diffusion coefficient for water becomes smaller at the higher levels of water uptake. We hope to address this issue in future work in which NMR measurements of the diffusion coefficient for water in epoxy are made.

Conclusions

In the T_{1xz} experiments, heterogeneity of mobility exists which is not primarily related to different sites within each monomer. The distance scale over which this heterogeneity of motion occurs is estimated by spin diffusion techniques to be about 4 nm. Therefore, cross-link density variations on a scale larger than 4 nm were not detected. Performing the experiments over a temperature range reduced the probability that variations in cross-link density on a scale larger than 4 nm were missed. Note that the mobility distinctions inferred from the T_{1xz} data may also have originated from heterogeneities in intermolecular packing in the glassy state.

A plot of the water chemical shift vs water content gave a linear relationship at fixed temperature (75 °C) and an intercept at zero water content of 2.48 ppm indicative of (a) a majority of water *molecularly dispersed* in the epoxy rather than aggregated in a water-like state within voids (i.e., if voids are present, they can only accommodate one or two water molecules) and (b) an absence of two sites of very different affinity (energetics) for water.

Line widths for water in an epoxy with relatively uniform water-concentration profiles have been measured as a function of water content. It was presumed that the foregoing data would be useful for detecting the presence of concentration gradients in a sample whose average water concentration is known. This latter expectation has not been confirmed experimentally, and reasons for this are not yet fully understood.

Finally, it is noted that the trend toward narrower water line widths at higher water concentrations indicates increased water mobility. This greater mobility is juxtaposed to the apparent reduction in *translational* mobility at higher water contents deduced from water uptake curves. Possible explanations for this were briefly considered based on a variety of observations reported in the literature.

References and Notes

(1) Apicella, A. Environmental Resistance of High-Performance Polymeric Matrices and Composites. In *International Encyclopedia of Composites*; Lee, S. M., Ed.; VCH Publishers: New York, 1990; Vol. 2, p 46.
(2) Moy, P.; Karasz, F. E. *Polym. Eng. Sci.* **1980**, *20*, 315.
(3) Schiering, D. W.; Katon, J. E.; Drzal, L. T.; Gupta, V. B. *J. Appl. Polym. Sci.* **1987**, *34*, 2367.
(4) Gupta, V. B.; Brahatheeswaran, C. *Polymer* **1991**, *32*, 1875.
(5) Gupta, V. B.; Drzal, L. T.; Lee, C. Y.-C.; Rich, M. J. *Polym. Eng. Sci.* **1985**, *25*, 812.
(6) Gupta, V. B.; Drzal, L. T.; Lee, C. Y.-C.; Rich, M. J. *J. Macromol. Sci. Phys.* **1985**, *B23*, 435.
(7) Gupta, V. B.; Drzal, L. T.; Lee, C. Y.-C.; Rich, M. J. *Polym. Prepr. (Am. Chem. Soc., Div. Polym. Chem.)* **1983**, *24*, 5.
(8) Bai, S. J. *Polymer* **1985**, *26*, 1053.
(9) Gupta, V. B.; Drzal, L. T.; Adams, W. W.; Omlor, R. *J. Mater. Sci.* **1985**, *20*, 3439.
(10) Jelinski, L. W.; Dumais, J. J.; Stark, R. E.; Ellis, T. S.; Karasz, F. E. *Macromolecules* **1983**, *16*, 1019.
(11) Ellis, T. S.; Karasz, F. E. *Polymer* **1984**, *25*, 664.
(12) Wong, T. C.; Broutman, L. J. *Polym. Eng. Sci.* **1985**, *25*, 521.
(13) Wong, T. C.; Broutman, L. J. *Polym. Eng. Sci.* **1985**, *25*, 529.
(14) Diamant, Y.; Marom, G.; Broutman, L. J. *J. Appl. Polym. Sci.* **1981**, *26*, 3015.
(15) Gupta, V. B.; Drzal, L. T.; Rich, M. J. *J. Appl. Polym. Sci.* **1985**, *30*, 4467.
(16) Certain commercial equipment, instruments, and materials are identified in this paper to adequately specify the experimental procedure. Such identification does not imply recommendation or endorsement by the National Institute of Standards and Technology, nor does it imply that the materials or equipment are necessarily the best available for the purpose.
(17) Rhim, W.-K.; Elleman, D. D.; Vaughan, R. W. *J. Chem. Phys.* **1973**, *59*, 3740.
(18) Mansfield, P.; Orchard, J.; Stalker, D. C.; Richards, K. H. B. *Phys. Rev.* **1973**, *B7*, 90.
(19) Rhim, W.-K.; Elleman, D. D.; Schreiber, L. B.; Vaughan, R. W. *J. Chem. Phys.* **1974**, *60*, 4595.
(20) Havens, J. R.; VanderHart, D. L. *Macromolecules* **1985**, *18*, 1663.
(21) Pham, Q. T.; Pétiaud, R.; Waton, H.; Llauro-Darricades, M.-F. *Proton and Carbon NMR Spectra of Polymers*; CRC Press Inc.: Boca Raton, FL, 1991; p 295.
(22) Bruker BVT1000 temperature controller manual, Bruker Instruments, Inc., Billerica, MA.
(23) Van Geet, A. L. *Anal. Chem.* **1970**, *42*, 679.
(24) Kaplan, M. L.; Bovey, F. A.; Cheng, H. N. *Anal. Chem.* **1975**, *47*, 1703.
(25) Vega, A. J.; Vaughan, R. W. *J. Chem. Phys.* **1978**, *68*, 1958.
(26) Vega, A. J.; English, A. D.; Mahler, W. *J. Magn. Reson.* **1980**, *37*, 107.
(27) Douglass, D. C.; Jones, G. P. *J. Chem. Phys.* **1966**, *45*, 956.
(28) Abragam, A. *Principles of Nuclear Magnetism*; Oxford University Press: London, 1961; Chapter 5.
(29) Schneider, W.; Pople, J. A.; Bernstein, H. J. *J. Chem. Phys.* **1958**, *28*, 601.
(30) Clemett, C. J. *J. Chem. Soc., Part A* **1969**, 455.
(31) Zelano, V.; Mirti, P. *Z. Phys. Chem.* **1983**, *138*, 31.
(32) Abragam, A. *Principles of Nuclear Magnetism*; Oxford University Press: London, 1961; Chapter 8.

MA946084B